Sudden switchover between the polyamorphic phase separation and the glass-to-liquid transition in glassy LiCl aqueous solutions

Yoshiharu Suzuki[a] and Osamu Mishima
National Institute for Materials Science, Namiki 1-1, Tsukuba, Ibaraki 305-0044, Japan

(Received 12 October 2012; accepted 4 February 2013; published online 25 February 2013)

Lithium chloride aqueous solutions (LiClaq solutions) below 10 mol.% are vitrified by cooling from room temperature to 77 K at 0.3 GPa. We examine the solvent state of the glassy sample and its transformation by heating at 1 atm using low-temperature differential scanning calorimetry and Raman spectroscopy. This experimental study suggests strongly that the solvent state of the glassy LiClaq solution closely relates to the state of high-density amorphous ice. Moreover, we reconfirm that the separation into the low-density amorphous ice and the glassy highly concentrated LiClaq solution occurs in the glassy dilute LiClaq solution at ∼130 K, not the glass-to-liquid transition which is commonly observed in the glassy LiClaq solution above ∼10 mol.%. In order to interpret the sudden switchover between the glass-to-liquid transition and the phase separation at ∼10 mol.%, we propose a state diagram of LiClaq solution which connects with a polyamorphic state diagram of pure water and discuss a possibility that the electric field induces a polyamorphic transition of water. © *2013 American Institute of Physics*. [http://dx.doi.org/10.1063/1.4792498]

I. INTRODUCTION

Recent studies of the super-cooled liquid water (H_2O) suggest that two liquid waters, low-density liquid water (LDL) and high-density liquid water (HDL), exist at low temperatures and that a liquid-liquid-critical point (LLCP) relating to the two waters exists.[1–3] This new concept for liquid water, so-called water polyamorphism, is important for understanding of the anomalous properties of low-temperature liquid water. For example, if the LLCP exists, the large fluctuations relating to two waters should generate around the LLCP. The anomalous properties of low-temperature liquid water may be caused by this dynamical fluctuation. However, it is difficult to examine experimentally the dynamics of liquid water around the LLCP because of the existence of crystallization region, so-called no-man's land.[1] In order to prevent the crystallization, the aqueous solution systems and the confinement in the form of solid materials with nano-sized pores have been used frequently and the dynamics of the low-temperature liquid water in their systems has been examined experimentally.[4–6] We believe that the reconsideration of the water in aqueous solution from the viewpoint of water polyamorphism has implication for the understanding not only of the anomalous properties of pure water but also of the structural and dynamical properties of the aqueous solution.[7–16]

Lithium chloride aqueous solution (LiClaq solution) is the most convenient material used to test the glassy solution experimentally and there are many experimental reports relating to the glassy LiClaq solution.[7,9,10,17–25] The experimental convenience lies in that the LiClaq solution with a concentration range above ∼9.0 mol.% forms easily a homogeneous glassy state by common cooling. However, it is difficult to vitrify the LiClaq solution below ∼9.0 mol.% homogeneously because of the partial crystallization of solvent water. Therefore, the structural relationship between the glassy pure water and the glassy aqueous solution is not clarified yet. We know that the homogeneous vitrification of LiClaq solutions depends strongly on the preparation conditions, for example, the cooling rate and the pressure.[7,23,24,26–28] Actually, it is possible to vitrify the pure water and the very dilute LiClaq solution at 1 atm using a liquid-hyperquenching method with a cooling rate of $\sim 10^6$ K/s.[7,26,27]

Previously, we vitrified the dilute LiClaq solutions at 1 atm using the liquid-hyperquenching method and examined their solvent state using Raman spectroscopy.[7] We suggested that the glassy dilute LiClaq solution is the inhomogeneous glass in which the low-density amorphous ice (LDA) and the glassy highly concentrated LiClaq solutions coexist. Moreover, we proposed that the dilute LiClaq solution separates to LDL and highly concentrated LiClaq solution during cooling and that this separation relates strongly to the liquid-liquid phase transition of pure water. On the other hand, we vitrified the LiClaq solutions in the concentration range from 2.0 to 10 mol.% by rapid cooling ($\sim 10^3$ K/s) at high pressure (0.3–0.5 GPa) and examined the solvent state using Raman spectroscopy.[10,24] This experimental result suggested that the glassy dilute LiClaq solution is similar to high-density amorphous ice (HDA) and is different from the glassy dilute LiClaq solution made by 1 atm-liquid-hyperquenching method. Moreover, when the glassy dilute LiClaq solution made by cooling at high pressure was heated at 1 atm, the LDA-like component appeared suddenly in the Raman spectrum.

In the present study, in order to clarify the relation between the amorphous ices and the glassy LiClaq solution, we examined in detail the solvent state in the glassy dilute LiClaq solution made by cooling at high pressure using low-temperature differential scanning calorimetry (DSC) and

[a]Electronic mail: suzuki.yoshiharu@nims.go.jp.

Raman spectroscopy. Moreover, we studied the change in the solvent state during heating at 1 atm. In this paper, we will discuss that the transformation of the solvent state in the glassy dilute LiClaq solution relates strongly to the water polyamorphism.

II. SAMPLES AND EXPERIMENTAL METHODS

A. Sample preparations

LiClaq solutions were prepared by mixing LiCl and ultra pure water (H_2O) (Direct-Q UV: Merck Millipore). The solute concentration ranged from 2.0 to 10.0 mol.% ($50 > R > 9$, where R stands for the number of water moles per mole of solute: $LiCl \cdot RH_2O$).

About 1 cm^3 of the solution was confined in an indium cup and was put in a steel piston-cylinder apparatus. After the sample was compressed to 0.3 GPa at room temperature, it was cooled down to 77 K at ~40 K/min. Subsequently, it was decompressed to 1 atm at 77 K and then was recovered.

For LiClaq solutions below 5.0 mol.%, to avoid the crystallization, the emulsified samples were used. The emulsion sample (1–10 μm in particle size) was made by stirring together a LiClaq solution (1 cm^3) and emulsion-matrix materials (methylcyclopentane: 0.75 cm^3, methylcyclohexane: 0.75 cm^3, and sorbitan tristearate: 50 mg).

To compare the solvent water in the glassy dilute LiClaq solutions with the HDA of pure H_2O, we made the HDA by the pressure-induced amorphization of hexagonal ice (ice I_h) at 77 K. Ultra-pure water was confined in an indium cup at 1 atm at room temperature and was put in a steel piston-cylinder apparatus. After the sample was cooled down to 77 K at 1 atm, it was compressed to 1.5 GPa. The amorphization of ice I_h started to occur around ~1.1 GPa. After the HDA was heated up to 160 K at 1.5 GPa for the structural relaxation of HDA,[29–32] it was cooled down to 77 K. Subsequently, it was decompressed to 1 atm at 77 K and then was recovered.

B. Differential scanning calorimetry

The low-temperature differential scanning calorimeter, DSC, (Perkin-Elmer, Pyris1) calibrated using both cyclopentane and *n*-heptane was used. About 25 mg of the glassy sample was packed in a handmade aluminum pan in liquid nitrogen and then the pan was put in the DSC apparatus. Unfortunately, it was difficult to measure the accurate weight of sample because of the packing of the sample in liquid nitrogen. The DSC scan was recorded upon heating from 93 K to a given temperature at 10 K/min in a flowing helium atmosphere.

In DSC measurement of general glassy materials, the heat generation caused by the structural relaxation hinders a pertinent observation of endothermic or exothermic changes relating to the important transition. In order to remove the effect of the structural relaxation, in this study, the sample was annealed repeatedly below the temperature at which the main transition occurred. Figure 1 shows the DSC scans for HDA, LDA, ice I_c, and ice I_h and the effects of the structural relaxation on the DSC scan. As shown in red thin DSC traces for HDA, the small but undeniable heat generation caused by the structural relaxation was observed below the HDA-to-LDA transition temperature (T_{LDA} ~120 K).[31,32] The structural relaxation was irreversible against the change of temperature.[30–32] We could minimize the influence of structural relaxation by repeat annealing below T_{LDA}, as shown by red thick DSC traces. Similarly, since the structural relaxation of LDA occurred,[32–34] the LDA was annealed repeatedly below the crystallization temperature, T_x, at which LDA crystallized to ice I_c and the influence of structural relaxation in LDA was minimized. (See blue DSC traces in Figure 1.)

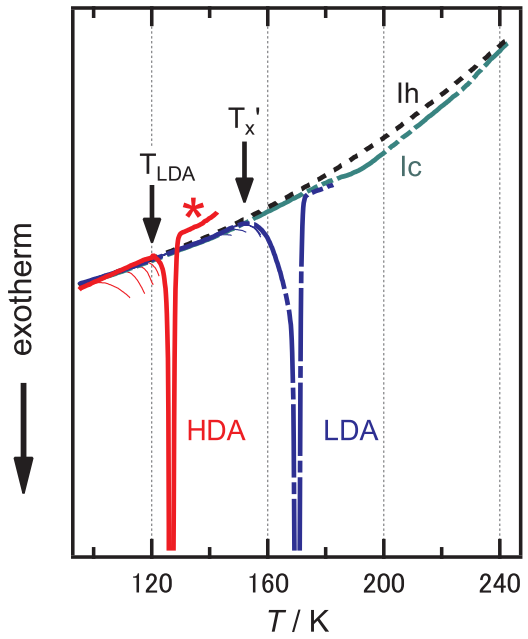

FIG. 1. Low-temperature DSC scans at 1 atm for HDA, LDA, ice I_c, and ice I_h of pure H_2O. The DSC scans for HDA, LDA, I_c, and I_h are represented by a red solid line, a blue dashed line, a green double-dashed line, and a black broken line, respectively. In order to remove the effect of structural relaxation of HDA and of LDA, HDA, and LDA were annealed repeatedly below T_{LDA} (~120 K) and below T_x' (~150 K), respectively. The DSC scans relating to the annealing treatment are drawn by thin lines. It is omitted to draw the bottom of exothermic peaks for the HDA-to-LDA transition and the crystallization of LDA. The red star represents the increase in heat flow of the LDA sample which is caused by the lowering of thermal contact between the sample and the pan.

In the DSC measurement for glassy LiClaq solution, it is hard to ignore the heat generation caused by the structural relaxation. Therefore, the glassy LiClaq solution was annealed repeatedly before the occurrence of the important transformation in this study. Here, we say that the structural relaxation of glassy LiClaq solution is not the core of a subject in this study. In order to discuss only the essential transitions intensively, hereafter, we will not display the DSC scans relating to the structural relaxation in the figures.

After the HDA-to-LDA transition in Figure 1, the value of heat flow for the LDA overshot as marked by a red star. We think that the overshooting of heat flow is caused by the lowering of the thermal contact between the sample and an aluminum pan due to the sudden volume increase. In order to remove the deviation from DSC trace after the HDA-to-LDA transition, we recovered the aluminum pan with LDA sample at 77 K from DSC apparatus after the HDA-to-LDA

transition, compressed by hand to reform the distorted sample in a mold and returned the aluminum pan in the DSC apparatus again. Therefore, it becomes difficult to discuss the absolute value of heat flow in DSC measurement exactly because of this recovery treatment of the sample and the imprecise measurement of sample weight. In this paper, therefore, we will discuss only the relative changes in the slope of DSC scans.

C. Raman spectroscopy

The polarized Raman spectra in the OH-stretching vibration range from 2800 to 3800 cm^{-1} were measured by using microscope Raman spectroscopy (Jovin Yvon T-64000). The resolution of the Raman spectrum was about 0.1 cm^{-1}. The incident laser was argon ion laser with wavelength of 488.0 nm and power of 500 mW at the source. The intensity of the Raman scattered radiation polarized parallel to the incident light, I_{VV}, was measured.

The intensity of the recorded Raman spectra was corrected by polarizer characteristics and back ground function. The corrected intensity was converted into the imaginary part of dynamical susceptibility as follows:

$$\chi''(\nu) = \frac{\kappa}{(\nu_L - \nu)^3}\left(1 - \exp\left(-\frac{hc\nu}{k_B T}\right)\right) I(\nu).$$

The ν stands for the Raman-shifted frequency written by cm^{-1} which is defined as $\nu = f/c$, where f is the frequency in Hz and c is the velocity of light. The ν_L is the incident laser frequency written by cm^{-1}, h is Planck's constant, k_B is Boltzmann's constant, and T is the absolute temperature. κ is the instrumental constant and is fixed to be unity.

The glassy LiClaq solutions and amorphous ices were placed in a cryostat with a temperature controller. In this study, the Raman spectra were recorded at 35 K at 1 atm.

III. RESULTS

The DSC scans for the glassy LiClaq solution of 6.3 mol.% ($R = 15$) made by cooling at 0.3 GPa are shown in Figure 2. There are two one-off exothermic peaks (A and B) and a reproducible increase in heat capacity (C) in the DSC scans. When the initial glassy sample is heated, the first exothermic event (A) occurs at ~130 K as shown in a red DSC trace. After this exothermic event is completed, the sample is cooled to 93 K rapidly and the second DSC measurement is carried out. In the "second" DSC scan (a blue DSC trace), the exothermic event is not observed around ~130 K and the increase in heat capacity (C) is observed at ~140 K. Subsequently, the large exothermic event (B) occurs at ~150 K. After the second exothermic event, the sample is cooled to 93 K again and the third DSC measurement is carried out. In the "third" DSC scan (a green DSC trace), the increase in heat capacity is observed again around ~140 K, and any exothermic event is not observed. The onset temperature of the increase in heat capacity agrees approximately with that in the second DSC scan.

The polarized OH-stretching vibrational Raman spectra for the glassy LiClaq solution of 6.3 mol.% made by the

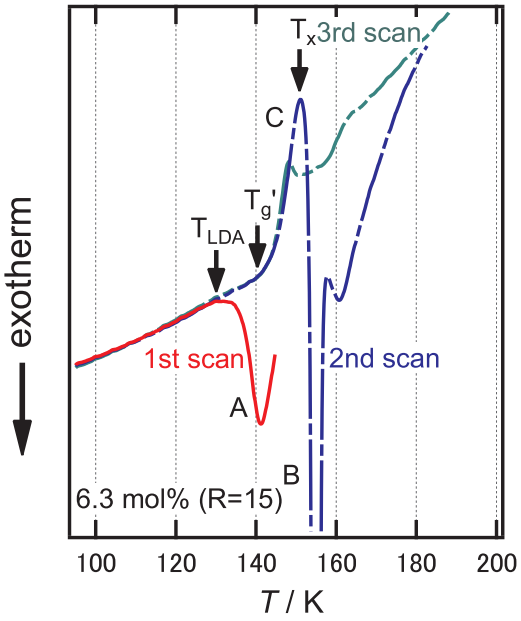

FIG. 2. Low-temperature DSC scans at 1 atm for the glassy LiClaq solution of 6.3 mol.% ($R = 15$) made by cooling at 0.3 GPa. The first DSC scan for the sample heated up to 145 K is displayed by a red solid line. The first exothermic event marked by A starts to occur around $T_{LDA} \sim 130$ K. The second DSC scan for the sample heated up to 183 K is displayed by a blue dashed line. The increase in heat capacity marked by C starts to occur around $T_g' \sim 140$ K, and subsequently the second exothermic event marked by B occurs around $T_x' \sim 150$ K. The third DSC scan for the sample heated up to 200 K is displayed by a green double-dashed line. The DSC scans relating to the annealing treatment are omitted.

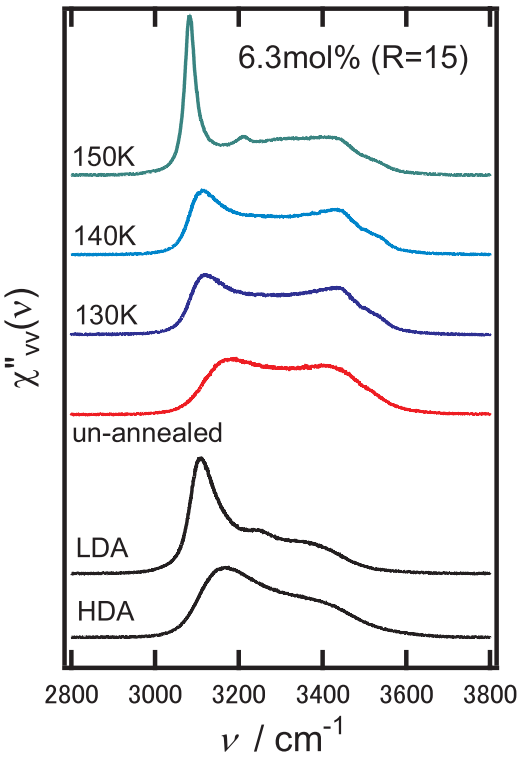

FIG. 3. The polarized Raman spectra, $\chi''_{vv}(\nu)$, of the OH-stretching vibrational mode for the glassy LiClaq solution of 6.3 mol.% ($R = 15$) made by cooling at 0.3 GPa. The sample was heated at 130, 140, and 150 K at 1 atm. All the Raman spectra were recorded at 35 K. The $\chi''_{vv}(\nu)$ for HDA and for LDA[30] are shown at the bottom.

cooling at 0.3 GPa are shown in Figure 3. After the glassy sample is heated up to a given temperature at 1 atm, the sample is cooled down to 35 K rapidly and the Raman spectrum is recorded. The Raman profile for the initial glassy sample (the un-annealed sample in Figure 3) is remarkably broad and is similar to that of HDA rather than that of LDA. The similarity in Raman profile between this glassy sample and HDA has been reported in our previous Raman study on the solvent water in the dilute LiClaq solutions (2.0–9.0 mol.%) vitrified using a pressure device developed for cooling the liquid materials rapidly under high pressure (0.3–0.5 GPa).[24,28]

When the glassy sample is annealed at 130 K at 1 atm, the transition occurs in the sample of the Raman measurement. Its state corresponds to the state of the sample after the first exothermic event in the DSC measurement. In the Raman spectrum for the sample heated up to 130 K, a relatively sharp peak, which is characterized by LDA, appears around $\sim$3100 cm^{-1}, suggesting that the first exothermic event relates to the transition of HDA to LDA. However, the temperature of the HDA-to-LDA transition, T_{LDA}, is $\sim$130 K and is different from the T_{LDA} for pure HDA (HDA of pure water) in Figure 1. The T_{LDA} for pure HDA is known to depend strongly on the relaxed state of pure HDA.[29] The T_{LDA} for the well-relaxed pure HDA is expected to be $\sim$136 K[29] and this value agrees with T_{LDA} for the glassy dilute LiClaq solution made by cooling at high pressure within experimental error. The high T_{LDA} for the glassy dilute LiClaq solution in the present experiment suggests that the existence of LiCl solute stabilizes the HDA state.

We observed the changes in the appearance of glassy sample by heating at 1 atm by a visual observation. The results are shown in Figure 4. The initial un-annealed glassy sample is transparent (Figure 4(a)). The sudden volume increase of the sample was observed during the first exothermic event and the increase ratio of volume was estimated to be about 20%, as recognized by comparison of sample size between Figs. 4(a) and 4(b). This sudden volume increase is similar to the volume increase at a transition of pure HDA to LDA.[35] The transparency of the sample after the first exothermic event does not change as shown in Figure 4(b).

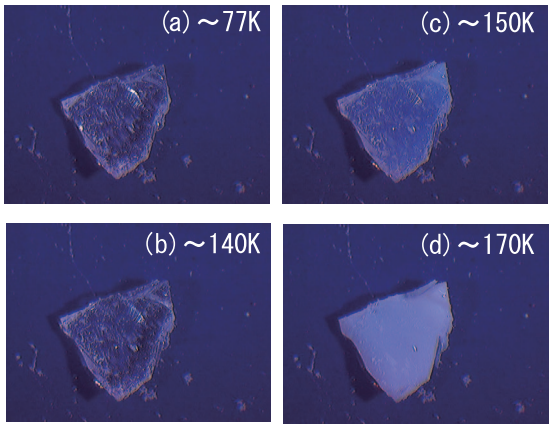

FIG. 4. Pictures of the glassy LiClaq solution of 6.3 mol.% ($R = 15$) made by cooling at 0.3 GPa. The sample ($\sim$3 mm) was heated from 77 to 170 K at 1 atm. The sample in (a) was the un-annealed sample at $\sim$77 K. The sample at $\sim$140 K in (b) corresponds to the sample after the first exothermic event. This sample is about 20% larger than the sample in (a). The sample at $\sim$150 K in (c) corresponds to the sample just after the second exothermic event. Its appearance starts to become opaque. The sample at $\sim$170 K has more clouded appearance.

The Raman profile of the sample heated up to 140 K (light blue line in Figure 3) is almost same with that of the sample heated up to 130 K (blue line). The state of the sample heated up to 140 K corresponds to the state of the sample after the increase in heat capacity of DSC measurement in Figure 2. This similarity in Raman spectra indicates that the topological molecular configurations in this sample do not change before and after the increase in heat capacity. This Raman result and the reproducibility of increase in heat capacity in DSC measurement suggest that the increase in heat capacity between 130–140 K relates strongly to the glass transition.

The Raman spectrum of the sample heated up to 150 K is represented by green line in Figure 3. The state of the sample heated up to 150 K corresponds to the state of the sample after the second endothermic event in the DSC measurement in Figure 2. In the Raman spectrum, a broad peak characterized by LDA disappears and a sharp peak characterized by crystalline ice I_c appears simultaneously. The onset temperature of the second exothermic event, which is estimated from the DSC scan in Figure 2, is $\sim$150 K and agrees roughly with the crystallization temperature, T_x, estimated from the DSC scan for pure LDA in Figure 1. Therefore, we think that the second exothermic event is caused by the crystallization of LDA component.

At the crystallization of LDA component in this sample, the appearance of sample begins to become opaque as shown in Figure 4(c). When the temperature rises further, the sample becomes more clouded (Figure 4(d)). Previously, a similar change in the appearance of glassy LiClaq solutions has been observed by Angell and Sare.[17] The increase in cloudiness by the heating may relate to the growth of the nuclei size of crystalline ice.

The DSC scans for the glassy LiClaq solutions of 3.2, 4.8, 6.3, 7.7, 9.1, and 10.0 mol.% (R = 30, 20, 15, 12, 10, and 9, respectively), which are made by cooling at 0.3 GPa, are shown in Figure 5. In all the DSC scans, the exothermic peak caused by the HDA-to-LDA transition, the increase in heat capacity caused by the glass transition and the exothermic peak cause by crystallization of LDA are observed. The onset temperature at which the first exothermic event relating to the HDA-to-LDA transition occurs (T_{LDA}), the onset temperature at which the increase in heat capacity occurs (T_g'), and the onset temperature at which the second exothermic event relating to the crystallization of LDA occurs (T_x') are plotted as a function of concentration in Figure 6. Additionally, the T_g for glassy highly concentrated LiClaq solutions above 10.0 mol.% made by cooling at 1 atm[18,21] are plotted in Figure 6. The T_{LDA} of pure HDA, which is prepared in this study, is represented by a red open square and the T_x of pure LDA is plotted by an open triangle. When the pure HDA relaxes by the annealing treatment, the T_{LDA} of HDA becomes higher.[29] The HDA seems to transform to LDA in temperature region marked by a hatch in Figure 6. According to the report by Handle *et al.*,[29] the T_{LDA} of well-relaxed HDA which is an-

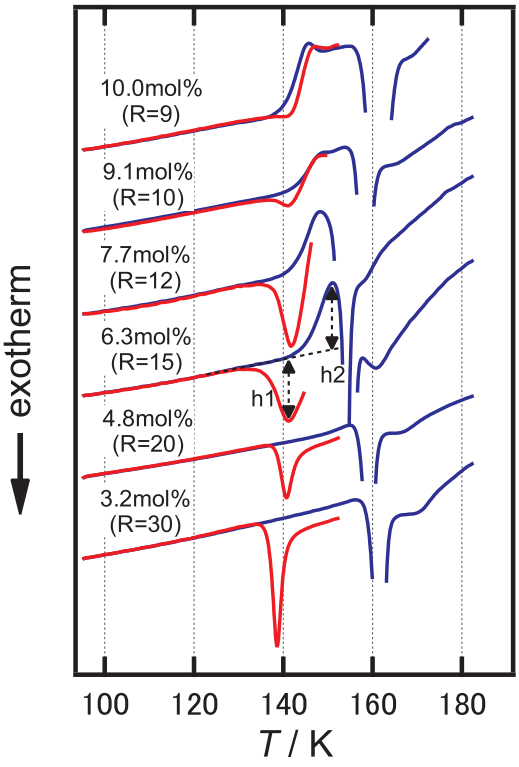

FIG. 5. Low-temperature DSC scans at 1 atm for the glassy LiClaq solutions of 10.0, 9.1, 7.7, 6.3, 4.8, and 3.2 mol.% (R = 9, 10, 12, 15, 20, and 30) which were made by cooling at 0.3 GPa. The first DSC scans for the sample heated up to the temperature slightly below the T_x' are displayed by red lines. The second DSC scans for the sample heated up to 183 K are displayed by blue lines. The LiClaq solutions of 4.8 and 3.2 mol.% are emulsified. The h_1 and h_2 stand for the depth of the first exothermic peak and the height of the increase in heat capacity, respectively. It is omitted to draw the bottom of exothermic peak for the crystallization.

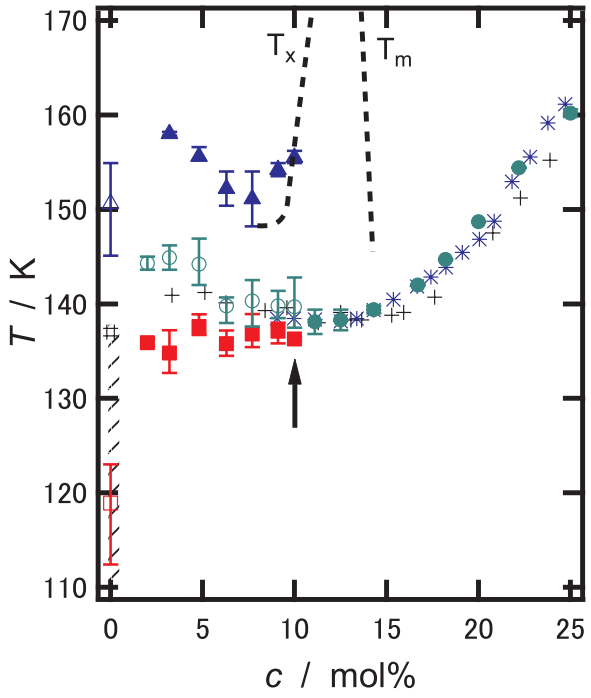

FIG. 6. The concentration dependences of T_g, T_{LDA}, T_g', and T_x' for the glassy LiClaq solutions. T_g stands for the glass-to-liquid transition temperature of glassy LiClaq solutions above 10.0 mol.% (blue asterisks in Ref. 18, black crosses in Ref. 21, and green filled circles in this work). T_{LDA}, T_g', and T_x' for the glassy dilute LiClaq solutions made by cooling at 0.3 GPa are represented by red filled squares, green open circles, and blue filled triangles, respectively. T_{LDA} for pure HDA (a red open square) and T_x for pure LDA (a blue open triangle) are plotted at 0 mol.%. T_{LDA} estimated from the HDA which is well-annealed at 0.1 GPa and 130 K[29] is represented by a black hash mark (#). The T_x and the melting temperature, T_m, for the glassy LiClaq solution, which were represented by broken lines, are referred from Ref. 21.

nealed at 130 K and 0.1 GPa for about 3 h is located in ∼136 K and is marked by a hash mark (#) in Figure 6.

IV. DATA ANALYSIS

We perform the linear combination analysis for the Raman spectrum of the glassy LiClaq solutions of 6.3 and 7.7 mol.% heated up to 130 K as the follows: $\alpha\ \chi''_{\mathrm{vv}}(\nu)_{\mathrm{LDA}} + (1-\alpha)\ \chi''_{\mathrm{vv}}(\nu)_{\mathrm{LiCl}}$, where $\chi''_{\mathrm{vv}}(\nu)_{\mathrm{LDA}}$ is the Raman spectrum of LDA, $\chi''_{\mathrm{vv}}(\nu)_{\mathrm{LiCl}}$, is the Raman spectrum of glassy LiClaq solution with different concentration between 10 and 25 mol.% and α stands for the ratio of LDA component. We have performed the same analysis in Ref. 7. As shown in Figure 7, both the Raman spectra can be reproduced well by the linear combination of the $\chi''_{\mathrm{vv}}(\nu)_{\mathrm{LDA}}$ and the $\chi''_{\mathrm{vv}}(\nu)_{\mathrm{LiCl}}$ for the glassy LiClaq solution of 10.0–11.1 mol.%. The result of the linear combination analysis using the $\chi''_{\mathrm{vv}}(\nu)_{\mathrm{LiCl}}$ for the glassy LiClaq solution with higher concentration than 11.1 mol.% is not good. This suggests that the LDA and the glassy LiClaq solution in the concentration ranges from 10 to 11 mol.% coexist in the glassy sample after the first exothermic event.

Now, if the glassy LiClaq solution of 6.3 mol.% separates perfectly and ideally into the pure LDA and the glassy LiClaq solution of 11.1 mol.%, we can estimate that the ideal ratio of pure LDA is 0.43 (= (11.1–6.25)/11.1). On the other hand, the ratio of LDA, α, calculated from the linear combination analysis in Figure 7(a) is ∼0.45 and this value agrees well with the ideal LDA ratio as shown above. Additionally, in the case of the glassy LiClaq solution of 7.7 mol.%, its ideal LDA ratio is 0.31 and the α calculated from Figure 7(b) is ∼0.32. Both the LDA ratios for the glassy LiClaq solution of 7.7 mol.% are almost same.

Next, we define the depth of the first exothermic peak, h_1, and the height of the increase in heat capacity, h_2, as shown in Figure 5 and roughly estimate a ratio of the separated LDA, $\Gamma = h_1/(h_1 + d \cdot h_2)$, where the coefficient d stands for a correction by the difference of the state in the glassy sample and is fixed to be unity in this study. Rigorously, we should adopt the peak area of the first exothermic transition which scales with mass instead of h_1 and should adopt the step height between a baseline before the glass transition onset and a baseline after the glass transition endpoint instead of h_2. However, it is difficult to estimate the exothermic peak area and the step height of heat capacity correctly because of the overlapping of the two exothermic peaks and the increase in heat capacity. Therefore, we attempt reluctantly the rough estimation of the ratio of LDA, Γ, using the values of h_1 and h_2. As shown in Figure 8, the change in Γ for the glassy sample above 6.4 mol.% seems to be linear and the intersection with the concentration axis is estimated to be 11–13 mol.% within

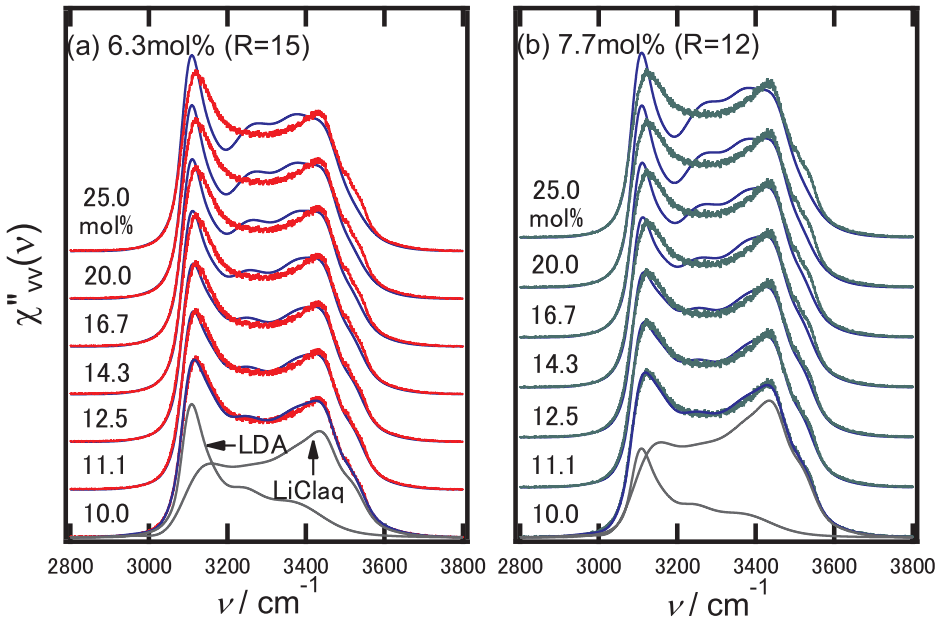

FIG. 7. The linear combination analysis of Raman spectra for the glassy LiClaq solutions heated up to 130 K. The $\chi''_{vv}(\nu)$s for the sample of 6.3 mol.% (red dots) and 7.7 mol.% (green dots) are shown in (a) and (b), respectively. These samples correspond to the samples after the first exothermic event in the DSC measurements. The linear combination analysis of $\chi''_{vv}(\nu)$ by the Raman spectrum for LDA, $\chi''_{vv}(\nu)_{LDA}$, and the Raman spectrum for the glassy LiClaq solution with various concentrations (10.0, 11.1, 12.5, 14.3, 16.7, 20.0, and 25.0 mol.%), $\chi''_{vv}(\nu)_{LiCl}$, are performed. The fitted spectra are represented by blue solid lines.

experimental errors. Considering that the LiCl solute hardly exists in LDA, this value indicates the concentration of the separated glassy LiClaq solution and becomes higher than the concentration of glassy sample before the phase separation. This rough estimation agrees with the result derived by the linear combination analysis of Raman spectra as mentioned before. On the other hand, the value of Γ for the emulsified samples below 4.8 mol.% deviates remarkably from the linear line in Figure 8. Since the h_1 and h_2 probably depend on the mass of sample and the mass of glassy LiClaq solution in the emulsified sample becomes less than the mass of the bulk sample, the deviation of Γ for the emulsified samples may be caused by the unrigorous definition of Γ.

We think that the increase in heat capacity after the first exothermic event relates to the glass-to-liquid transition of the separated glassy LiClaq solution. Although there is no experimental evidence that the separated glassy sample transforms to liquid, we infer that the glass transition relates to a transform from glass to liquid. A ratio of the height of the increase in heat capacity to the first exothermic peak becomes larger with the increase in concentration of glassy sample as shown in Figure 8. This correlation suggests that the increase in heat capacity is caused by only the glassy LiClaq solution. From another point of view, we conclude that the increase of heat capacity does not relate to the glass transition of the separated LDA. Furthermore, as discussed in above paragraphs, the glassy highly concentrated LiClaq solution exists in the sample after the first exothermic event. The glass-to-liquid transition of the glassy highly concentrated LiClaq solution has been well established.[17,18] From these circumstantial evidences, we judge that the increase in heat capacity in DSC scan relates to the glass-to-liquid transition of the separated glassy LiClaq solution.

V. DISCUSSION

From several results shown above, we derive two conclusions: (i) the solvent state in the glassy dilute LiClaq solution made by cooling at 0.3 GPa is very similar to the state of HDA and (ii) when the glassy dilute LiClaq solution is heated at 1 atm, the phase separation into the LDA and the highly

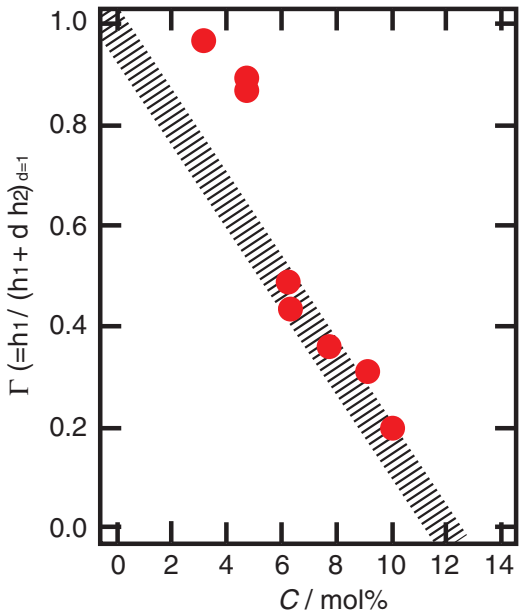

FIG. 8. The concentration dependence of Γ. Γ is defined as $h_1/(h_1+d\cdot h_2)$, where h_1 and h_2 is the depth of the first exothermic peak and the height of the increase in heat capacity in DSC scans of Figure 5, respectively. The coefficient d is fixed to be unity. A broken gray line is drawn for the guide of eyes.

concentrated LiClaq solution occurs. This phase separation of dilute aqueous solution is consistent with the results proposed by Angell and Sare.[17,18]

In the case of the glassy LiClaq solutions above ~10 mol.%, when the glassy sample is heated at 1 atm, the glass-to-liquid transition is observed first, not the phase separation.[18,21] The values of T_g for the glassy LiClaq solutions above ~10 mol.% become lower with the decrease of concentration as shown Figure 6. For example, the T_g for the glassy sample of 10 mol.% is ~135 K. For the glassy dilute LiClaq solutions below 10 mol.%, however, the glass-to-liquid transition is not observed around 135 K, instead the phase transition to LDA is observed first. The glass-to-liquid transition in high concentration ranges seems to switch smoothly, but suddenly, to the phase separation in the low concentration ranges as shown in Figure 6.

We consider that the sudden switchover between the glass-to-liquid transition and the phase separation around 10 mol.% correlates to the liquid-liquid transition of pure water as shown in a schematic state diagram of Figure 9. Considering that the effect of electrolyte solute on the liquid water is equivalent to the effect of pressure[36–38] and that the high-pressure liquid water corresponds to HDL,[1,28] the HDL (HDA) at high pressure regions in the *P-T* plane of pure water (0 mol.%) will be equivalent to the solvent water of the LiClaq solution at high concentration regions in the *C-T* plane at 1 atm as shown by a large arrow in Figure 9. Our present conclusion that the solvent state of glassy dilute LiClaq solution made by cooling at 0.3 GPa is similar to HDA is reasonable as shown by the sample preparation path (red broken line) in the *P-C-T* state diagram. A similar relation between the

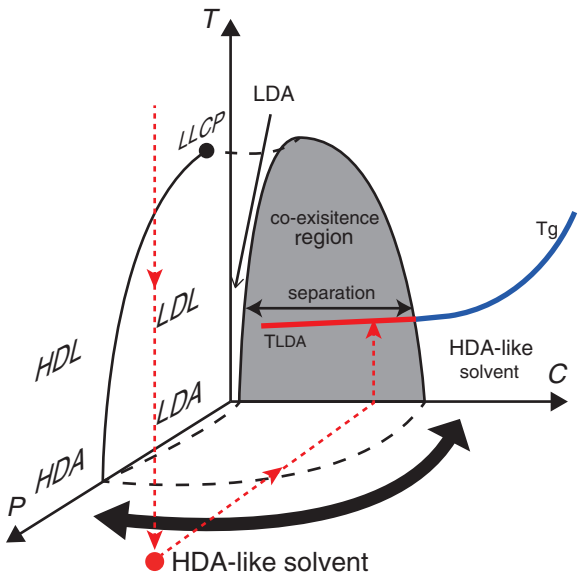

FIG. 9. Schematic pressure-concentration-temperature (*P-C-T*) state diagram of LiClaq solution. The sample preparation path and the experimental path in this work are shown by red broken lines. HDL (or HDA) at high pressures in the *P-T* plane is equivalent to the solvent water in LiClaq solution in high concentrations range in the *C-T* plane as shown by a thick arrow. The co-existent line of LDL and HDL in the *P-T* plane may correspond to the co-existent region of LDL and highly concentrated LiClaq solution in the *C-T* plane. The phase separation into the LDA and the glassy highly concentrated LiClaq solution (red line) occurs in the co-existence regions.

HDA and the hydration in aqueous solution has been pointed out already.[38–40] On the other hand, the co-existence curve of LDL and HDL in the *P-T* plane may correspond to a co-existence region (a dome in Figure 9) of LDA and HDA-like solvent water at lower concentration ranges in the *C-T* plane at 1 atm. The sudden switchover between the glass-to-liquid transition and the phase separation around 10 mol.% may be induced by the existence of the co-existent region such as shown in Figure 9.

Murata and Tanaka[4] have asserted that the transition of HDA to LDA occurs above the T_g and the transition to LDA may relate to the growth of LDA nuclei or the spinodal decomposition. In our present experiment, the glass-to-liquid transition of the glassy dilute LiClaq solution occurs and the HDA-like solvent water changes to the HDL-like solvent water (Figure 10(a)). Simultaneously, the LDL (LDA) nuclei may be created because of the low viscosity of HDL-like solvent water (Figure 10(b)). The size of LDL (LDA) nuclei may be shorter than wavelength of light because of the transparency of sample in Figure 4(b). We think that the glass-to-liquid transition of the glassy dilute LiClaq solution may correspond to the lower glass transition of double glass transitions appearing in glassy dilute LiClaq solutions under pressure that have been reported by Kanno.[20] Actually, we observe the subtle increase in heat capacity just before the transition to LDA, though the height of the increase in heat capacity is various each time we measure. Moreover, in simultaneous measurements of the sample temperature and the sample volume of glassy dilute LiClaq solutions during heating, the subtle increase in heat capacity and the increase of sample volume occur simultaneously and, soon after that, the temperature increase is observed.[9,10] The simultaneous occurrence of the subtle increase in heat capacity and the increase of sample volume suggests a possibility that the glass-to-liquid transition (Figure 10(a)) and the transition to LDA accompanying with the volume increase (the creation of LDA nuclei in Figure 10(b)) may occur simultaneously. We think that the volume change and the heat generation, which are caused by the transition to LDA, should occur at the same time. However, the rise in temperature caused by the transition to LDA appears later than the increase in volume[9,10] because of the overlapping of the heat generation induced by the creation of LDA nuclei, the heat absorption induced by the (quasi-)adiabatic expansion of sample, the complex heat behavior (generation and absorption) relating to the structural relaxation of glassy LiClaq solution which is made by cooling under high pressure, and so on.

On the other hand, the solvent water near an ion resembles HDA and is remarkably stable because of strong electrostatic interaction between the ion and the water molecule.[25] Therefore, the solvent water near the ion hardly transforms to the LDA-like structure. (Figure 10(b)) We propose that when a part of solvent water in the glassy dilute LiClaq solution transforms to LDA-like solvent above T_g, the ions coated by the HDA-like water may be excluded from the area of LDA, and then may be cooperatively assembled each other as shown in Figure 10(c). Moreover, the assembly of the ion coated by HDA-like water may be re-vitrified because of the increase of concentration. Although, there is no direct

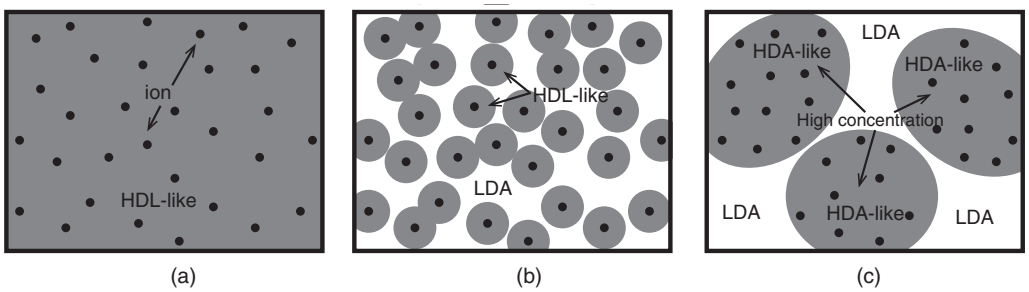

FIG. 10. Schematic drawings of the phase separation process in the glassy dilute LiClaq solution. (a) The glassy dilute LiClaq solution made by cooling at 0.3 GPa is homogeneous glass and its solvent water (gray regions) resembles HDA. The ion particles are represented by black points. Above T_g of the glassy dilute LiClaq solution, the HDA-like solvent change to the HDL-like solvent. (b) The portion of HDL-like solvent water transforms to LDA immediately at the T_g. However, the HDL-like solvent water near an ion hardly changes to LDA because of the strong electrostatic interaction. (c) The ions coated by HDL-like water may be excluded from LDA-like solvent water and then may be assembled cooperatively. The re-vitrification of the assembly of ions coated by HDL-like water may occur because of the increase of concentration.

experimental evidence for both the cooperative aggregation of the ions coated by HDL-like water and the re-vitrification of the assembly of the ions coated HDA-like water, the existence of both the Raman profile relating to glassy highly concentrated LiClaq solution as shown in Figure 7 and the reproducible increase in the heat capacity relating to glassy highly concentrated LiClaq solution as shown by DSC scans in Figs. 2 and 5 suggest the existence of domains of glassy highly concentrated LiClaq solution which have been proposed in Ref. 14. We expect the future studies relating to the dynamics of the phase separation occurring in the glassy dilute aqueous solutions.

It appears feasible that the extrapolation of T_{LDA} for the glassy dilute LiClaq solutions to 0 mol.% connects to the T_{LDA} (~136 K) for well-relaxed HDA[29] as shown in Figure 6. This suggests that, if the state of HDA connects thermodynamically with the solvent state of dilute LiClaq solution, the glass-to-liquid transition of pure HDA at 1 atm will occur above 136 K. The reason is that the glass transition for glassy dilute LiClaq solutions is not observed in the temperature ranges below ~136 K in this study. The studies relating to the glass transition of pure HDA is carried out actively by Loerting group in Innsbruck University.[29,41,42] In this stage, the location of T_g for HDA is not clarified yet and the glass-to-liquid transition of HDA is under discussion.[29,41–43]

VI. REMARKS

As for the similarity of effect on liquid water between ion concentration and pressure as suggested by Refs. 36–40, our present and previous studies suggest that the HDA-like solvent water adjacent to the ion seems to be relatively stable. Previously we have compared the solvent water in glassy LiClaq solutions with the relaxed HDA and suggested that the state of solvent water far from the ion and the state of solvent water adjacent to the ion are similar to the HDA relaxed at low pressure and the HDA relaxed at high pressure, respectively, as shown in an inset of Figure 11.[25] In other words, changing the viewpoint from ion concentration to "electric field," the state of water applied by the strong electric field is similar to the state of water under high pressure and the state of water applied by weak electric field is similar to the state of water under low pressure. This speculation provides a new relation that the effect of "electrostatic field" on water may be equivalent to the effect of pressure[44,45] as shown by a thick arrow in the schematic diagram of Figure 11. In short, it may be able to induce the polyamorphic transition of water by the application of "electric field." We infer that the transformation of crystalline ice to HDA by the electron beam irradiation[46] might be induced by the electric field of electron beam. We expect that the relation between the electrostatic field and the water polyamorphism will be understood in the future study.

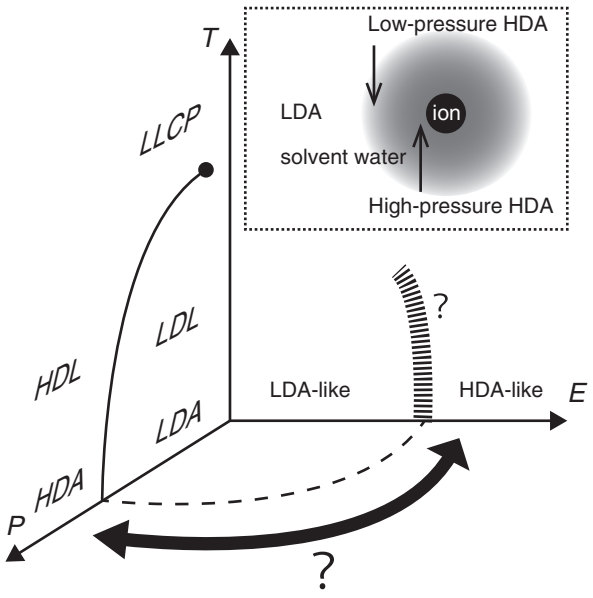

FIG. 11. Schematic pressure-"electric field"-temperature (*P-E-T*) state diagram of pure water. The schematic drawing in an inset represents that the water adjacent to an ion resembles the high-pressure HDA and the water far from the ion is similar to the low-pressure HDA.[25] Considering that the electrostatic field strength becomes weak so as to go away from the ion, the effect of electric field on water may be equivalent to the effect of pressure as shown by a thick arrow. This suggests a possibility that the liquid-liquid transition of water might be induced by the application of "electric field."

ACKNOWLEDGMENTS

We thank D. Gembris for letting us know Ref. 44.

[1]O. Mishima and H. E. Stanley, Nature (London) **396**, 329 (1998).
[2]P. G. Debenedetti, J. Phys. Condens. Matter **15**, R1669 (2003).
[3]P. H. Poole, U. Essmann, F. Sciortino, and H. E. Stanley, Phys. Rev. E **48**, 4605 (1993).
[4]K. Murata and H. Tanaka, Nature Mater. **11**, 436 (2012).
[5]L. Liu, S. H. Chen, A. Faraone, C. W. Yen, and C. Y. Mou, Phys. Rev. Lett. **95**, 117802 (2005).
[6]M. Oguni, Y. Kanke, A. Nagoe, and S. Namba, J. Phys. Chem. B **115**, 14023 (2011).
[7]Y. Suzuki and O. Mishima, Phys. Rev. Lett. **85**, 1322 (2000).
[8]Y. Suzuki, Chem. Phys. Lett. **335**, 357 (2001).
[9]O. Mishima, J. Chem. Phys. **123**, 154506 (2005).
[10]O. Mishima, J. Chem. Phys. **126**, 244507 (2007).
[11]D. Paschek, Phys. Rev. Lett. **94**, 217802 (2005).
[12]S. Chatterjee and P. G. Debenedetti, J. Chem. Phys. **124**, 154503 (2006).
[13]D. Corradini, M. Rovere, and P. Gallo, J. Chem. Phys. **132**, 134508 (2010).
[14]L. Le and V. Molinero, J. Phys. Chem. A **115**, 5900 (2011).
[15]D. Russo, J. Teixeira, L. Kneller, J. R. D. Copley, J. Ollivier, S. Perticaroli, E. Pellegrini, and M. A. Gonzalez, J. Am. Chem. Soc. **133**, 4882 (2011).
[16]E. G. Strekalova, D. Corradini, M. G. Mazza, S. V. Buldyrev, P. Gallo, G. Franzese, and H. E. Stanley, J. Biol. Phys. **38**, 97 (2012).
[17]C. A. Angell and E. J. Sare, J. Chem. Phys. **49**, 4713 (1968).
[18]C. A. Angell and E. J. Sare, J. Chem. Phys. **52**, 1058 (1970).
[19]H. Kanno and C. A. Angell, J. Phys. Chem. **81**, 2639 (1977).
[20]H. Kanno, J. Phys. Chem. **91**, 1967 (1987).
[21]B. Prével, J. F. Jal, J. Dupuy-Philon, and A. K. Soper, J. Chem. Phys. **103**, 1886 (1995).
[22]K. Winkel, M. Seidl, T. Loerting, L. E. Bove, S. Imberti, V. Molinero, F. Bruni, R. Mancinelli, and M. A. Ricci, J. Chem. Phys. **134**, 024515 (2011).
[23]M. Kobayashi and H. Tanaka, J. Phys. Chem. B **115**, 14077 (2011).
[24]Y. Suzuki and O. Mishima, J. Chem. Phys. **117**, 1673 (2002).
[25]Y. Suzuki and Y. Tominaga, J Chem. Phys. **134**, 244511 (2011).
[26]G. P. Johari, A. Hallbrucker, and E. Mayer, Nature (London) **330**, 552 (1987).
[27]E. Mayer, A. Hallbrucker, G. Sartor, and G. P. Johari, J. Phys. Chem. **99**, 5161 (1995).
[28]O. Mishima and Y. Suzuki, J. Chem. Phys. **115**, 4199 (2001).
[29]P. H. Handle, M. Seidl, and T. Loerting, Phys. Rev. Lett. **108**, 225901 (2012).
[30]Y. Suzuki and Y. Tominaga, J. Chem. Phys. **133**, 164508 (2010).
[31]Y. P. Handa, O. Mishima, and E. Whalley, J. Chem. Phys. **84**, 2766 (1986).
[32]K. Winkel, E. Mayer, and T. Loerting, J. Phys. Chem. B **115**, 14141 (2011).
[33]Y. Suzuki and O. Mishima, J. Phys. Soc. Jpn. **72**, 3128 (2003).
[34]G. P. Johari, A. Hallbrucker, and E. Mayer, Science **273**, 90 (1996).
[35]O. Mishima, L. D. Calvert, and E. Whalley, Nature (London) **314**, 76 (1985).
[36]R. Leberman and A. K. Soper, Nature (London) **378**, 364 (1995).
[37]S. E. McLain, S. Imberti, A. K. Soper, A. Botti, F. Bruni, and M. A. Ricci, Phys. Rev. B **74**, 094201 (2006).
[38]J. Holzmann, R. Ludwig, A. Geiger, and D. Pascheck, Angew. Chem. Int. Ed. **46**, 8907 (2007).
[39]M. P. Longinotti, M. A. Carignano, I. Szleifer, and H. R. Corti, J. Chem. Phys. **134**, 244510 (2011).
[40]H. R. Corti, F. J. Nores-Pondal, and C. A. Angell, Phys. Chem. Chem. Phys. **13**, 19741 (2011).
[41]M. Seidl, M. S. Elsaesser, K. Winkel, G. Zifferer, E. Mayer, and T. Loerting, Phys. Rev. B **83**, 100201(R) (2011).
[42]O. Mishima, J. Chem. Phys. **121**, 3161 (2004).
[43]O. Andersson and A. Inaba, J. Phys. Chem. Lett. **3**, 1951 (2012).
[44]X. Hu, N. Elghobashi-Meinhardt, D. Gembris, and J. C. Smith, J. Chem. Phys. **135**, 134507 (2011).
[45]J. L. Aragones, L. G. MacDowell, J. I. Siepmann, and C. Vega, Phys. Rev. Lett. **107**, 155702 (2011).
[46]H. G. Heide, Ultramicroscopy **14**, 271 (1984).